Available online at www.sciencedirect.com
SCIENCE DIRECT®

ELSEVIER

PALAEO

Palaeogeography, Palaeoclimatology, Palaeoecology xx (2006) xxx – xxx

www.elsevier.com/locate/palaeo

Paleohydrology of an Upper Aptian lacustrine system from northeastern Brazil: Integration of facies and isotopic geochemistry

J.D.S. Paz [a], D.F. Rossetti [b,*]

[a] *Universidade Federal do Pará, Centro de Geociências, Campus do Guamá S/N Belém-PA, Brazil*
[b] *Instituto Nacional de Pesquisas Espaciais-INPE Rua dos Astronautas 1758, Jardim da Granja, CP 515 São José dos Campos, Cep 12245-970 São Paulo, Brazil*

Received 29 March 2004; received in revised form 6 October 2005; accepted 24 March 2006

Abstract

The Codó Formation records the initial evolutionary stages of an intracontinental rift system formed along the Brazilian equatorial margin in the Late Aptian. Deposits of this unit exposed on the eastern margin of the Grajaú Basin include gypsum, bituminous black, shales and limestones. These lithologies were formed in a low energy, well stratified, anoxic and hypersaline lake system developed in a dominantly arid/semi-arid climate. This lacustrine succession is internally organized into three categories of shallowing-upward cycles, with the first- and second-order cycles being related to seismic activity associated with fault reactivations, and the third-order cycles recording climatic fluctuations. Studies emphasizing petrography and analysis of the geochemical tracers Fe, Mg, Sr, Mn, Na and Ca helped to identify the sedimentary facies that kept a primary signal, which were thus appropriate for isotopic investigations aiming paleoenvironmental and paleohydrologic reconstructions. The results of this study revealed a wide distribution of dominantly low carbon and oxygen isotope values in carbonates, ranging from −5.69‰ to −13.02‰ and from −2.71‰ to −10.80‰, respectively. This paper demonstrates that at least in the particular case of oxygen, the isotope ratios vary according to seismically-induced shallowing-upward cycles, with values in general lower at their bases, where central lake deposits dominate, and progressively higher upward, where marginal lake deposits are more widespread. In addition to confirming a depositional signature for the analysed samples, this behavior allowed the development of a seismic-induced isotope model. These lighter isotope ratios appear to be related to flooding events promoted by subsidence, which resulted in the development of a perennial lake system, while heavier isotope values are related to ephemeral lake phases favored by uplift and/or increased stability. Furthermore, the results show that a closed lake system dominated, as indicated by the overall good positive covariance (i.e., +0.42 to +0.43) between the carbon and oxygen isotopes, though open phases are also recorded by negative covariance values of −0.36. During closed phases, the $\delta^{18}O$ displayed the highest range of variation (i.e., −3.63‰ to −4.89‰) due to increased residence time, while this variation was low (i.e., −0.09‰ to −1.87‰) during open lake phases, when there was a balance in the water isotope composition maintained by continuous basin inflow.

Keywords: Paleohydrology; Isotopes; Paleolake; Aptian; Late Aptian; Northeastern Brazil

1. Introduction

$\delta^{13}C$ and $\delta^{18}O$ records have been successfully used for reconstructing the evolution and circulation patterns of oceanic basins throughout the geological time (e.g.,

* Corresponding author. Tel.: +55 12 39456451; fax: +55 12 39456488.
E-mail address: rossetti@dsr.inpe.br (D.F. Rossetti).

0031-0182/$ - see front matter © 2006 Elsevier B.V. All rights reserved.
doi:10.1016/j.palaeo.2006.03.040

Abell and Williams, 1986; Charisi and Schmitz, 1995; Hendry and Kalin, 1997). These studies are mostly based on the principle that the organic matter in marine sediments is characterized by extremely uniform isotopic compositions, which vary according to climate, as well as oceanic hydrology and limnology. The interpretation of these geochemical indicators in lacustrine settings is more complex, mostly because lake environments are more diverse, as evidenced by a wider distribution of carbon isotope ratios ranging from −25.9‰ to −10.5‰ (Bird, 1991). Since the pioneer work of Stuiver (1970), several studies of modern and Quaternary lake systems have provided the basis for discussing the many parameters that might influence the isotopic composition of the total inorganic carbon dissolved in lake waters (e.g., Katz et al., 1977; Anderson and Arthur, 1983; McKenzie, 1985; ~~Hil-laire-~~Marcell and Casanova, 1987; Bellanca et al., 1989; Gasse et al., 1989; Talbot and Kelts, 1990; Rosenmeier et al., 2002; Herczeg et al., 2003; Russell et al., 2003). Despite these efforts, distinguishing among the mechanisms that lead to variations in isotope composition of lake waters is not straightforward, as local causes might be mistaken by externally forced environmental changes (Talbot, 1990). In addition, in contrast to marine and modern lacustrine systems, the record of chemical changes in ancient lake deposits is yet very limited (Bird, 1991; Lister et al., 1991; Szulc et al., 1991; Camoin et al., 1997; In Sung and Kim, 2003), and this has precluded a wider use of these geochemical tracers for paleoenvironmental purposes. Therefore, geochemical analyses from a larger range of lacustrine analogs where local causes can be distinguished from those of regional scale are still needed in order to provide a full understanding of the mechanisms controlling lacustrine carbonate sedimentation.

Despite the complex response, the available information concerning carbon and oxygen isotope variations has arrived at some important generalizations. The most significant one for paleoenvironmental interpretation was the recognition of a covariance of these geochemical tracers in hydrologically closed lake systems, as opposed to a non-covariance in inlet lakes (e.g., Eicher and Siegenthaler, 1976; Gasse et al., 1987; Gasse et al., 1989; Talbot, 1990; Talbot and Kelts, 1990). Carbon and oxygen isotopes have been also applied for climate reconstructions of lake systems (e.g., Talbot and Kelts, 1990; Lister et al., 1991; Valero-Garcés et al., 1995). These applications are, however, highly dependent on a full understanding of facies distribution and of the possible modifications occurred during burial.

The goal of this paper is to contribute to the documentation of $\delta^{13}C$ and $\delta^{18}O$ values in ancient lacustrine systems, and discuss the causes of variations in these values by analysing their relationship with shallowing-upward cycles within an Upper Aptian succession formed during the early stages of a passive marginal rift. This unit, represented by the Codó Formation, is well exposed in several quarries along the eastern margin of the Grajaú Basin, where detailed studies focusing facies and facies architecture, stratigraphy, petrography, as well as Sr and S isotopes, have provided a basis to support ~~the conclusion of~~ deposition in a dominantly lacustrine setting (e.g., Rossetti et al., 2000; Paz and Rossetti, 2001; Rossetti et al., 2004). An integrated approach combining facies and isotope geochemistry provides the basis to analyse the distribution of carbon and oxygen isotopes in this ancient lake system, as well as to investigate the main parameters controlling the lake hydrology.

2. Geological setting

The Codó Formation records the first deposits accumulated within a broad and shallow depression formed by mild tectonic stretching before the main rifting stage that culminated with the formation of the Equatorial South Atlantic Ocean during the Albian. These deposits are well represented in the Grajaú Basin (Fig. 1A), a semi-graben formed by combination of pure shear stress and strike–slip deformation (Azevedo, 1991; Góes and Rossetti, 2001). This rift, which is connected to the São Luís Basin in the north, became an aborted intracontinental structure as the continental break up migrated northward.

The sedimentary fill of the São Luís-Grajaú Basin (Fig. 1B) reaches up to 4000 m in the depocenters, and consists chiefly of Cretaceous deposits organized into three depositional sequences, i.e., S1, S2 and S3, formed during the Late Aptian/Early Albian, Early/Middle Albian and Middle Albian/Late Cretaceous, respectively (Rossetti, 2001). The lowermost sequence S1 contains the Codó Formation, subject of this paper, and represents a succession up to 450 m thick of sandstones, gypsum, shales and limestones. This sequence displays a tripartite subdivision into systems tracts (Rossetti, 2001), with the lowstand systems tract consisting of deposits that grade progressively southward from shallow marine to continental (i.e., fluvial, deltaic, and lacustrine). These are overlain by strata formed in the transgressive systems tract, which consists of a wedge of richly fossiliferous (mostly bryozoa, echinoderm, foram

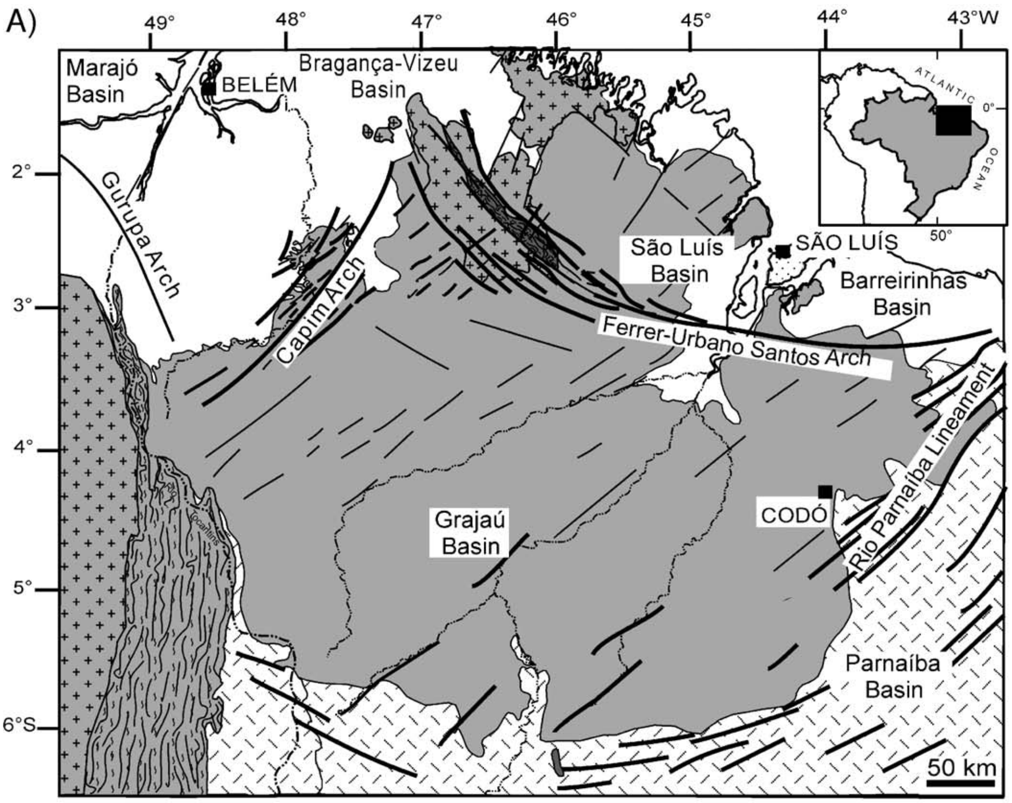

B) STRATIGRAPHY OF THE SÃO LUÍS- GRAJAÚ BASIN

AGE	Depositional Sequence	STRATIGRAPHIC UNIT North	South	Tectonic stage
Quaternary		Post-Barreiras Deposits		Passive Margin
Late Miocene?		Barreiras Formation (II)		
Early Miocene?		Barreiras Formation (I)	Pirabas Formation	
Early Tertiary?	Sequence 3	Cujupe Formation	Itapecuru Group	Drift
Cenomanian		Alcântara Formation		
Middle/Late Albian	Sequence 2	Undifferentiated Unit		Rift
Early Albian Late Aptian	Sequence 1	Codó Formation	Grajaú Formation	Pre-rift

Fig. 1. (A) Location of the study area in the Codó region, eastern margin of the Grajaú Basin. (B) Stratigraphy and main tectonic stages of the São Luís-Grajaú Basin.

and dinoflagellate) shales that pinches out to the basin margins. The highstand systems tract consists of shallow marine to continental deposits typically displaying stratal patterns varying upward from aggradational to progradational.

The maximum thickness of the Codó Formation in the Grajaú Basin is 150 m (Rezende and Pamplona, 1970). Its paleontologic content mostly includes pollen, continental ostracods, insects, and fish, which are all in agreement with a dominantly lacustrine depositional system. Pollen data allowed the establishment of a precise late Aptian age with basis on the presence of *Sergipea variverrucata* (Batista, 1992; Lima, 1982; Rossetti et al., 2001). The Codó Formation either grades downward into fluvial and deltaic deposits of the Grajaú Formation (e.g., Mesner and Wooldrigde, 1964), or sharply overlies an unconformity over older Paleozoic and Triassic basement rocks. Its upper contact is an unconformity with Albian shallow marine, green to brownish-red mudstones interbedded with fine- to very fine-grained, cross-stratified sandstones of the Itapecuru Group (e.g., Rossetti and Truckenbrodt, 1997; Rossetti et al., 2001).

3. Facies architecture and depositional system

The detailed facies analysis and characterization of the cyclic nature of the Codó Formation exposed in the eastern margin of the Grajaú Basin have been previously reported elsewhere (e.g., Paz and Rossetti, 2001, 2005). However, a summary of the main descriptions and interpretations will be provided in the following, as they are critical to understand the carbon and oxygen isotope signals.

3.1. Description

The Codó Formation consists of a lacustrine succession up to 25 m thick. In the eastern margin of the basin, this unit displays deposits attributed to three main sub-environments (Fig. 2): (1) central lake deposits, consisting of gypsum and bituminous black shales; (2) transitional lake deposits, represented by laminated argillites and limestones, and occasionally, massive sandstone; and (3) marginal lake deposits, including massive blocky pelites, fenestral calcarenites, ostracodal and pisoidal limestones, rhythmites of limestones and microbial mats, as well as tufas. Paleosols, karstic features, meteoric cement and vadose pisoid, typical of subaerial and/or meteoric exposure, are frequent in the marginal lake deposits.

Three categories of cycles have been recognized in this unit (Fig. 3). Third-order cycles consists of millimetric interbeddings (individual beds are usually <5 to 10 mm thick), encompassing facies that vary according to the position in the lake setting. Hence, the central lake deposits show interbeddings either of bituminous black shales and gypsum, or bituminous black shales with streaks of lime-mudstone and bituminous black shales with lenses of native sulphur. The transitional lake deposits display bituminous black shale interbedded with peloidal limestone or green to gray laminated argillites interbedded either with lime-mudstone or peloidal wackestone–packstone. The marginal lake deposits show either green to gray laminated argillites and ostracodal wackestone to grainstone, as well as alternations of ostracodal and/or lime mudstones, microbial mats and vadose pisoidal packstones.

Second-order cycles consist of either complete or incomplete successions with upward transitions from central to marginal lake deposits, with the latter displaying high internal facies variability when comparing one cycle to another. These cycles are characterized by limited lateral extension, as well as frequent and random thickness changes, which vary from few cm up to 5 m.

First-order cycles define four episodes of shallowing (Fig. 4), organized from bottom to top as units 1 to 4. Unit 1 is only partly exposed at the base of the sections, consisting of bituminous black shales interbedded with lime-mudstones, and are attributed to central and transitional lake settings. Unit 2 reaches up to 8 m thick and contains, at the base, black bituminous shales interbedded with gypsum, which grade upward into limestones, laminated argillites and massive block pelites displaying a variety of features related to transitional and marginal lake settings. The gypsum is, in general, absent or occurs only as millimetric lenses or isolated crystals of gypsum. Unit 3 reaches up to 4 m thick and is constituted by transitional and marginal lake deposits similar to the underlying unit, but with an increased frequency of the latter. A remarkable and exclusive feature of this unit 3 is the presence of oolites and calcareous (i.e., ostracodal packstone) concretions in its upper portions, which constitute important stratigraphic markers. The uppermost unit 4 is up to 5 m thick, being represented by laminated argillites containing only thin (<1 mm thick) laminae of gypsum or lime-mudstone.

The first-order cycles closely match with stratigraphic horizons displaying syn-sedimentary soft sediment deformation that occur between undeformed deposits (Fig. 4), an observation that was crucial for revealing their genesis. Hence, units 1 and 2 correspond respectively to undeformed strata and deformation zones 1 and 2 described in Rossetti and Góes (2000). Deformation zone 1 consists of spar-filled cracks interconnected with small-scale faults, fissures and stylolites inclined at a high angle to bedding. Deformation zone 2 consists of strata with complex convolute folds associated with thrust faults, pseudonodules, and mound-and-sag structures, the latter corresponds to synclines and anticlines mantled by sigmoidal laminations

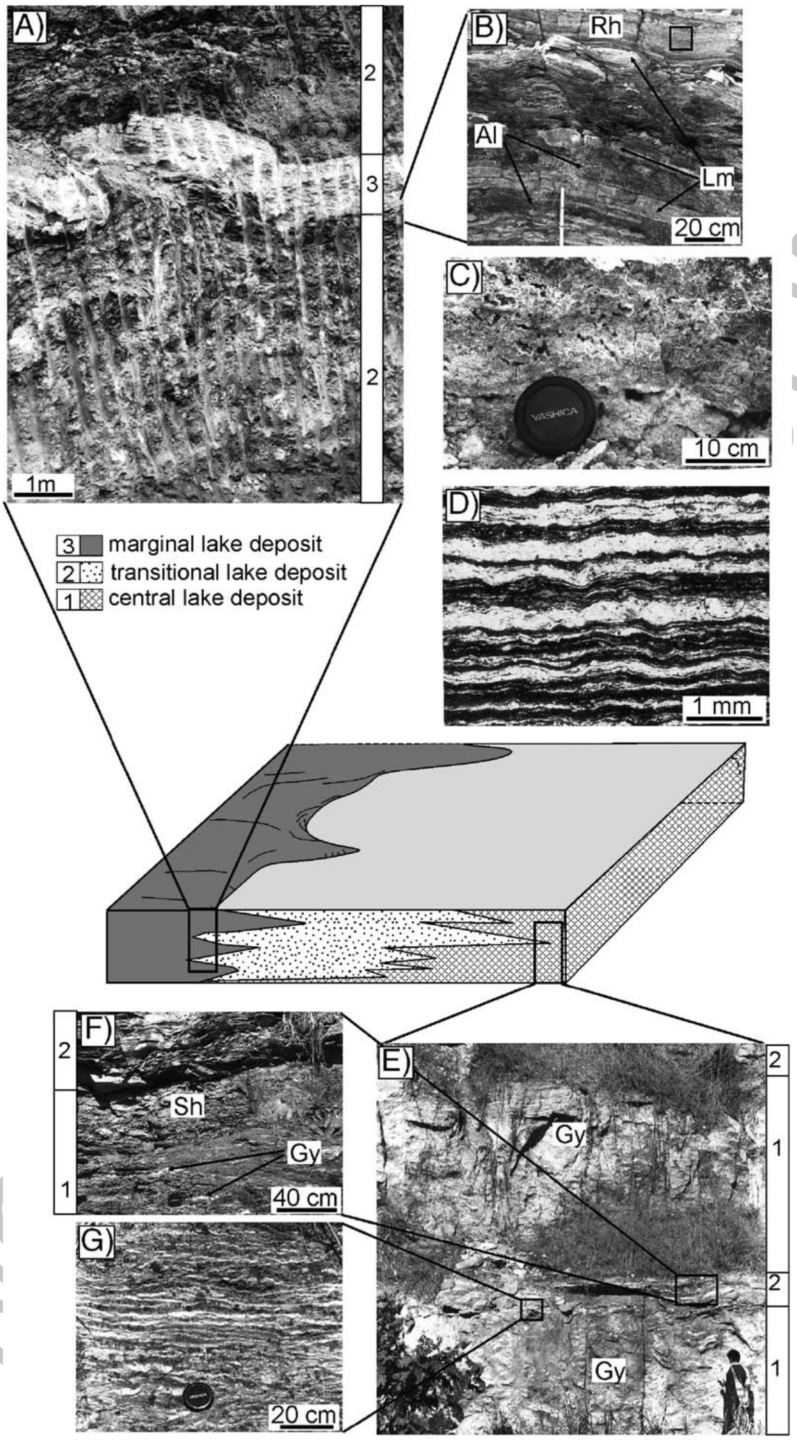

Fig. 2. Diagram illustrating the proposed lacustrine depositional model for the Codó Formation, characterized by central to marginal lake deposits. (A) General view of marginal lake deposits between transitional lake deposits. (B) A detail showing the upward gradation from interbedded limestones (Lm) and laminated argillites (Al; transitional lake) to rhythmites (Rh; marginal lake). (C) Fenestral calcarenite from marginal lake deposits. (D) Rhythmite of limestones (lighter color) and microbial mats (darker color) from marginal lake deposits. (E) General view of central lake deposits (Gy = gypsum). (F) Bituminous black shales (Sh) interbedded with gypsum (Gy) (person for scale = 1.70 m tall). (G) Laminated gypsum (lens cap = 10 cm in diameter).

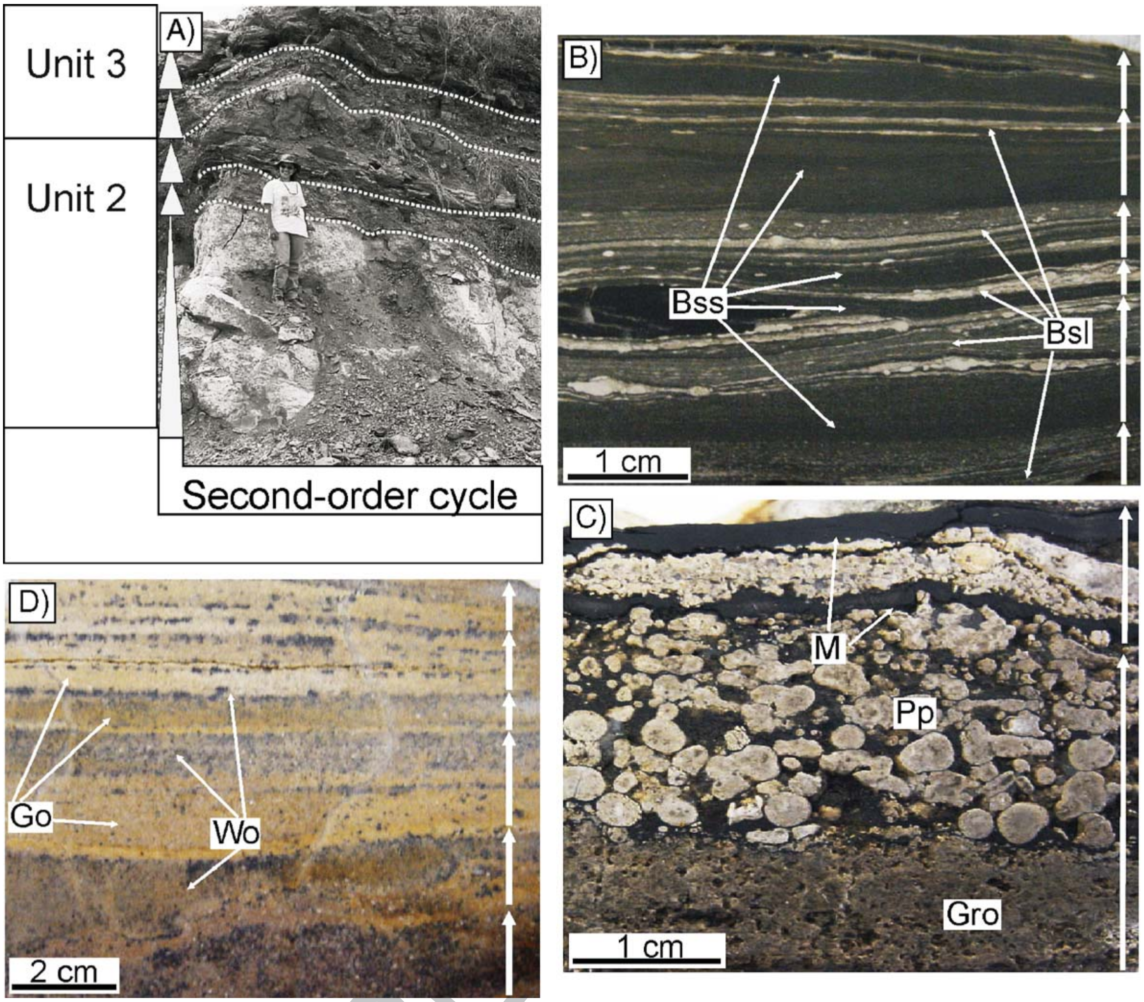

Fig. 3. Shallowing-upward cycles of the Codó Formation. (A) Examples of first- and second-order cycles (person for scale = 1.50 m tall). (B–D) Third-order cycles formed by alternations of bituminous black shale with streaks of lime-mudstone (Bsl) and bituminous black shales with native sulphur (Bss) (B), ostracodal grainstone (Gro) and vadose pisoidal packstone (Pp) with microbial mats (M) (C), ostracodal grainstone (Go) and wackestone (Wo) (D).

inclined toward the sag centers. Unit 3 is equivalent to deformed strata with normal faults and fissures that are vertical to near vertical, present ragged morphologies with small, delicate edges, and taper both downward and upward after a few centimeters, being associated with intraformational boulders up to 2.5 m long. The uppermost unit 4 consists of shales with irregular convolute folds.

3.2. Interpretation

The several facies described in the Codó Formation are attributed to a low energy, well stratified, anoxic and hypersaline lake system developed under a dominantly arid/semi-arid climate (Paz and Rossetti, 2001). The third-order cycles record minor changes in depositional conditions, which resulted in packages comprising alternations between mud settling and chemical precipitation of gypsum or limestones. This characteristic, added to the regular thickness variation, is consistent with climatic fluctuations, with individual laminae reflecting mud deposition and chemical precipitation taking place during less and more arid phases, respectively.

The higher-order cycles seem to have a different origin. The second-order cycles record successive episodes of upward gradation from deeper to relatively shallower lake environments, resulting in superposition of marginal lake deposits upon transitional and/or central lake deposits. The high facies variability when

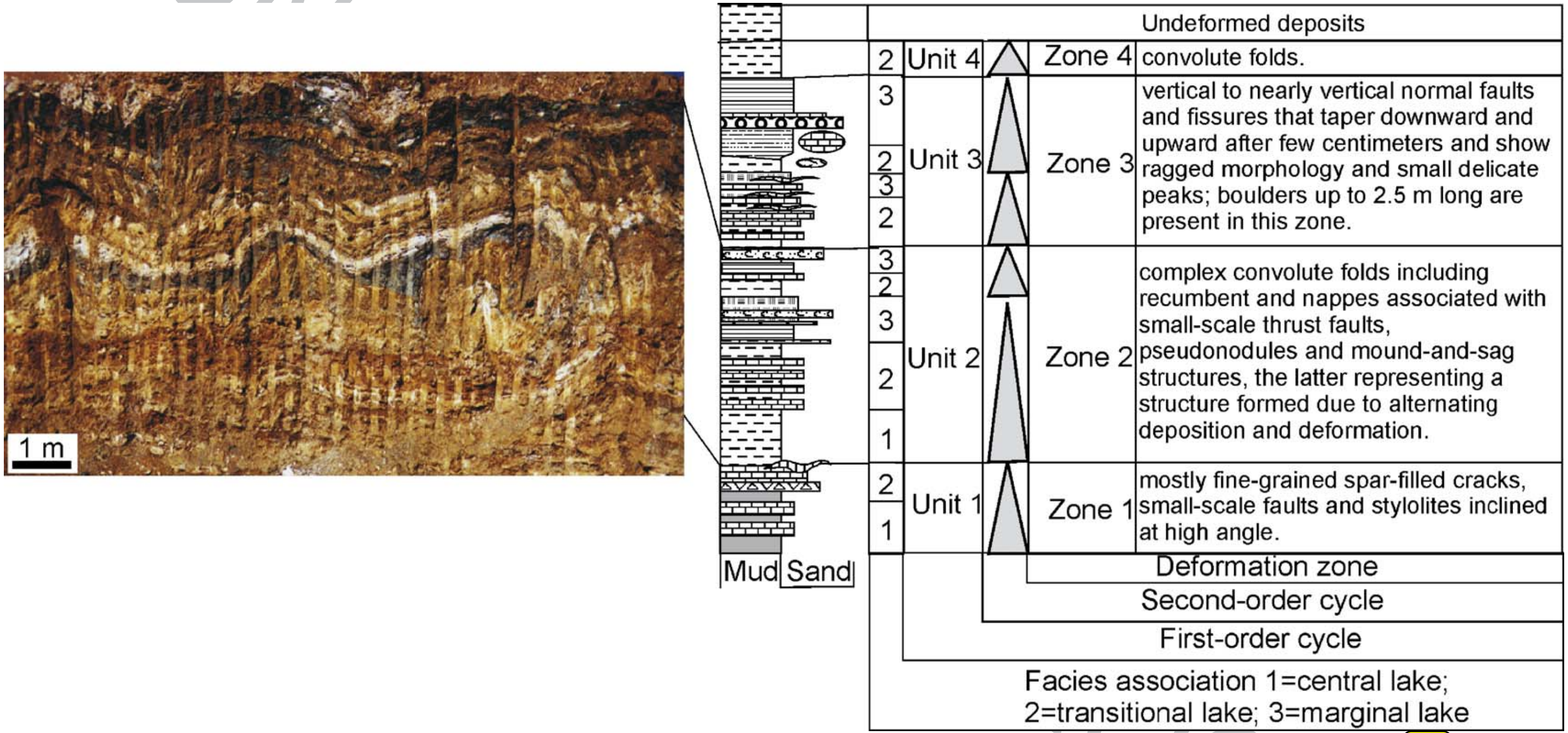

Fig. 4. First- and second-order cycles of the Codó Formation with relation to soft-sediment deformation zones attributed to syn-sedimentary seismic activity (see Fig. 7 for legend).

comparing one cycle to another, the limited lateral extension and the frequent and random thickness variations are attributes that match better with tectonically driven (e.g., Martel and Gibling, 1991; Benvenuti, 2003), rather than more regular climatic cycles (e.g., Olsen, 1986; Goldhammer et al., 1990; Smoot and Olsen, 1994; Steenbrink et al., 2000).

The first-order cycles also appear to have resulted from syn-sedimentary tectonics (Fig. 4), as suggested by their good correlation with deformation zones attributed to contemporaneous seismic activity related to fault reactivation (Rossetti and Góes, 2000). Based on this fact, it has been proposed that the Codó lake system was affected by alternating periods of extension and even compression (Paz and Rossetti, 2005). The prevalence of central lake deposits at the base of the first-order cycles would have formed during higher subsidence, promoted by extension. On the other hand, the more widespread distribution of marginal lake deposits in the top of these cycles would record periods of higher stability or uplift. In addition to affecting the development of the shallowing-upward cycles, these processes appear to have had a strong control on the isotope evolution of this lake system, as discussed in this paper.

4. Experimental methods

^{13}C and $\delta^{18}O$ data were obtained from freshly exposed samples along quarries to guarantee they were free from influence of modern weathering. Although these isotopes are more commonly measured from fossils, the analyses were performed here using whole-rock limestones due to the fact that only ostracods are present in the studied deposits, and their distribution is not uniform to provide a good record of the individual cycles throughout the succession. Stable isotopic analysis has been successfully performed in whole-rock carbonates (e.g., Camoin et al., 1997). According to these authors, this type of sample has the advantage of minimizing possible deviations related to

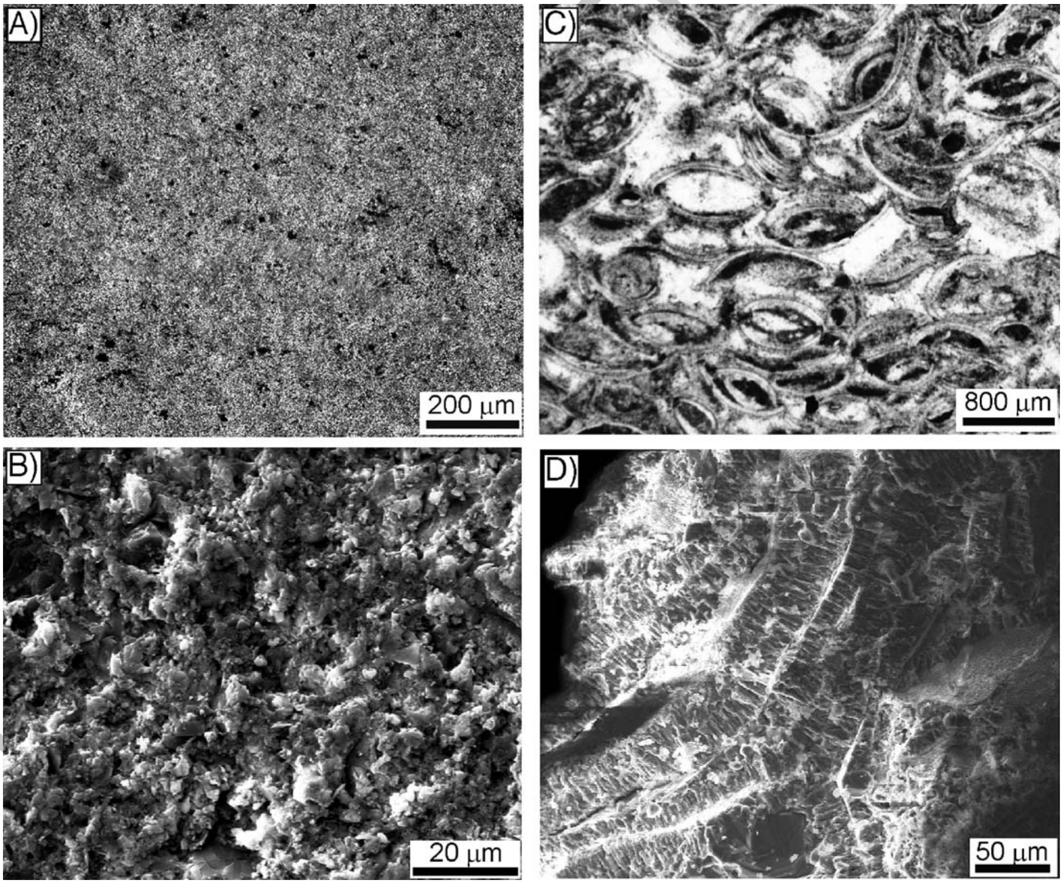

Fig. 5. Photomicrographies of nondiagenetically modified samples utilized for isotopic analysis. (A, B) Lime-mudstone (A = crossed nichols; B = scanning electron microscopy). (C) Ostracodal grainstone (crossed nichols). (D) Electron micrography illustrating ostracod shells of ostracodal grainstone, formed by densely-packed, columnar calcite crystals of primary origin.

vital effects, and even diagenesis. Twenty milligrams of powered sample reacted in vacuum with 100% of orthophosphoric acid at 25 °C during 12 h. The released CO_2 and H_2O were captured with liquid N_2. The CO_2 was separated from the water with a solution of alcohol and acetone in an off-line gas extraction line, and thereafter taken to the VG Isotech SIRA II mass spectrometer in the Stable Isotope Laboratory at the Universidade Federal de Pernambuco (LABISE/UFPE). The results are reported in δ notation, which is defined as the per mil deviation from the Viena Peedee Belemnite Standard (‰ V-PDB). Analytical data were normalized to the NBS-20 sample standard. Replicate analysis gave a standard deviation (2σ) lower than 0.02‰ for $\delta^{13}C$ and 0.03‰ for $\delta^{18}O$.

It is noteworthy to comment that the decision to undertake the present carbon and oxygen work was made only after that detailed petrographic, SEM, as well as strontium and sulphur isotope studies, had supported a primary lacustrine origin for the gypsum associated to the limestones (Paz et al., 2005). This study led to suspect that the limestones interbedded with the primary gypsum also had a great potential to preserve their depositional characteristics. In order to eliminate the diagenetic influence, the limestones were evaluated petrographically, with the analyses being undertaken using selected facies displaying primary characteristics.

Furthermore, the trace elements Fe, Mg, Mn, and Sr were also analysed in order to better detect any possible diagenetic imprint. This procedure consisted in drying 1.5 g of sample at 1000 °C for 2 h, fusing them afterwards with lithium tetraborate and lithium fluorite, and analysing by X-ray fluorescence spectrometer.

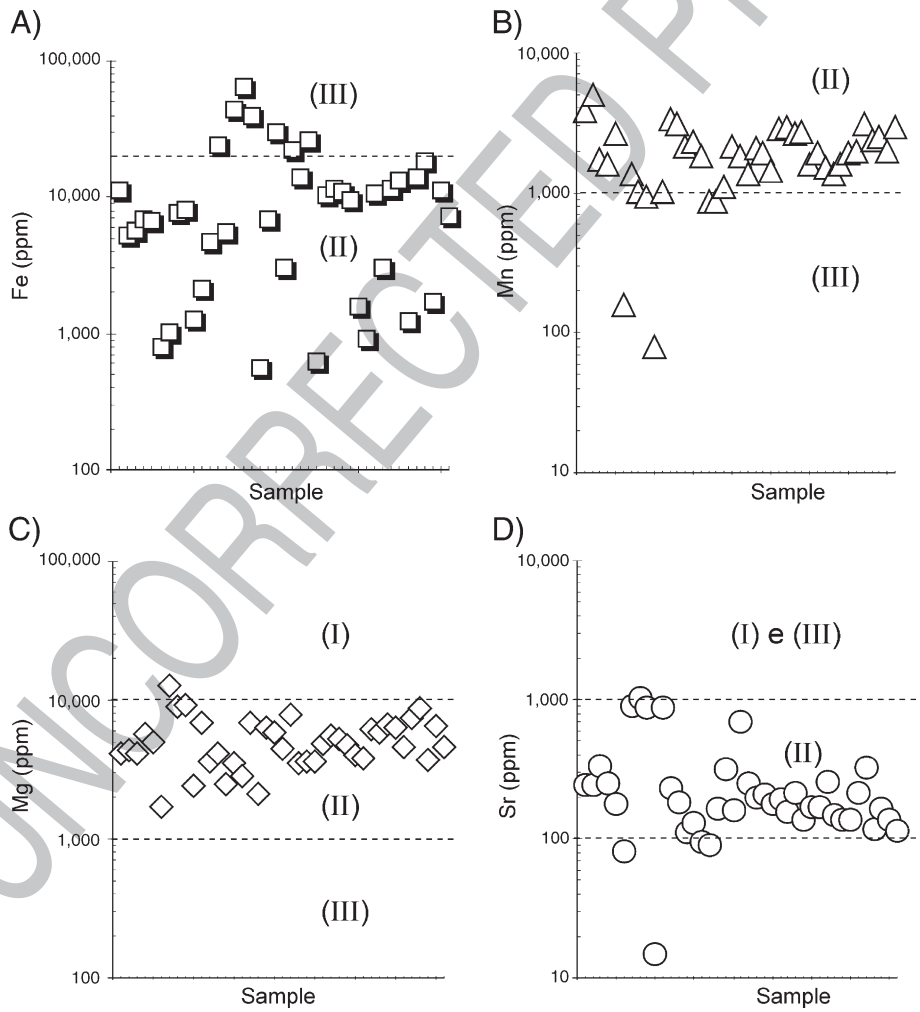

Fig. 6. Distribution of the trace elements Fe (A), Mn (B), Mg (C), and Sr (D) in the analysed samples (I = marine calcite; II = continental calcite; III = diagenetic calcite; after Tucker and Wright, 1990).

5. Evaluation of diagenetic overprint

Petrographic analysis of 83 limestone samples from the Codó Formation allowed an evaluation of diagenetic changes by observing the amount of lime mud, recrystallization, replacement, cementation, and fracturing. Several authigenic processes were observed, the most important ones including recrystallization of calcite, cementation and filling of fractures and secondary porosity by mosaics of calcite, replacement of micrite and ostracod shells by chert and chalcedony, and pyrite formation either within ostracod shells or dispersed in the lime-mudstones. Despite these modifications, it was possible to select 53 samples consisting of microfacies either not affected or only mildly affected by diagenesis, which enhanced their potential to preserve a primary carbon and oxygen composition. The samples used in this study included mostly lime-mudstone (36%) and ostracodal wackestone to grainstone (45%; Fig. 5), and subordinately fenestral calcarenite (8%), pisoidal packstone (6%), and peloidal packstone to grainstone (6%).

Geochemical analyses of the trace elements Fe, Mg, Mn, and Sr helped to corroborate that the selected samples were not significantly modified after deposition. These elements are the main tracers in the calcite structure of both marine and non-marine limestones. Considering that their values remained constant through time, which seems to have been the case at least for most of the Phanerozoic (Holland, 1978), a comparison among values commonly expected from stratal waters provides information for detecting potentially significant diagenetic influences. The results (Fig. 6) show that, in general, all the samples that appeared to be petrographically suitable for isotope analysis contain geochemical tracers in proportions expected for continental deposits not affected by diagenesis. Exceptions are a few samples displaying high Fe content, though these were also included in the isotope analysis presented here, considering that: (1) the other geochemical tracers are within the range expected for diagenetically non-affected rocks; (2) the isotope values do not show any divergence with respect to the other samples; and (3) they derive from facies that have high volume of

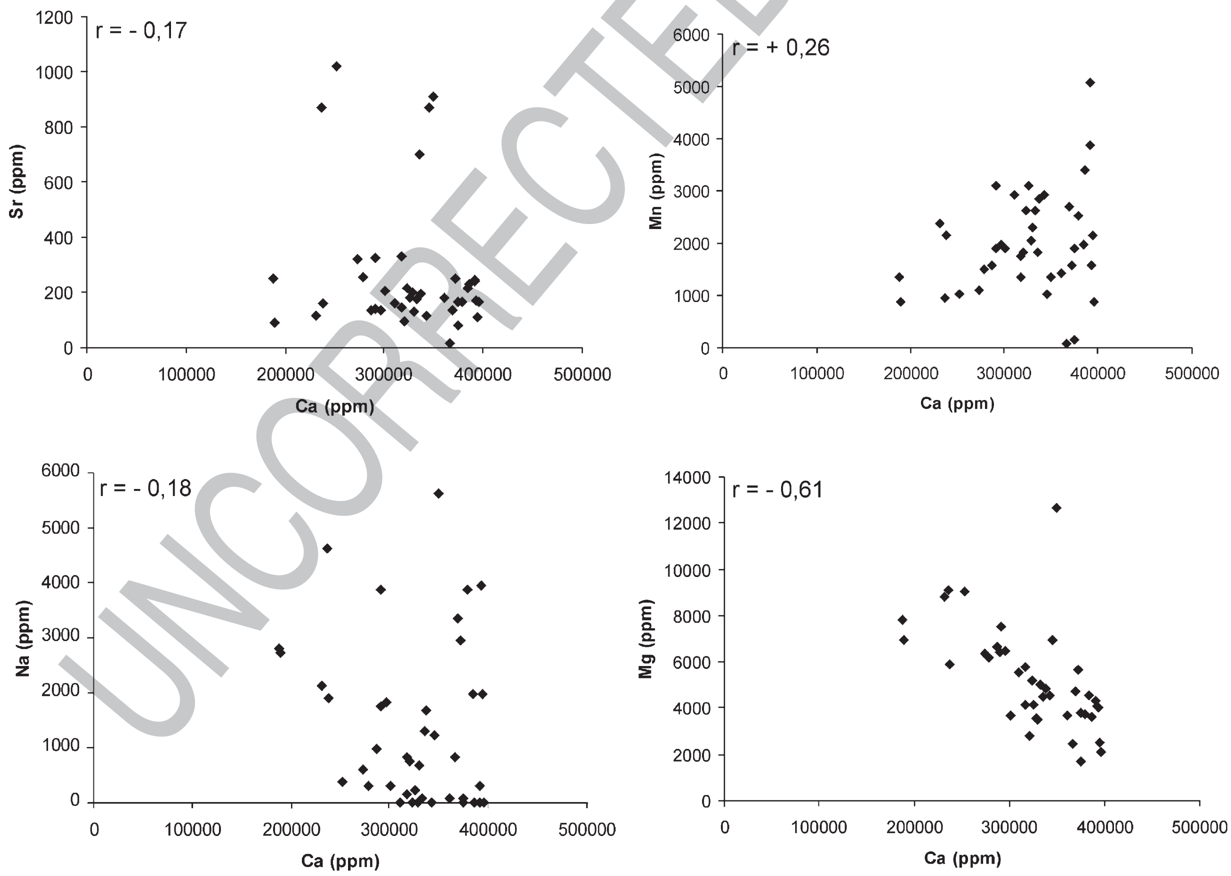

Fig. 7. Binary diagrams of the trace elements Sr, Mn, Na and Mg against Ca, with the correspondent correlation coefficient (*r*).

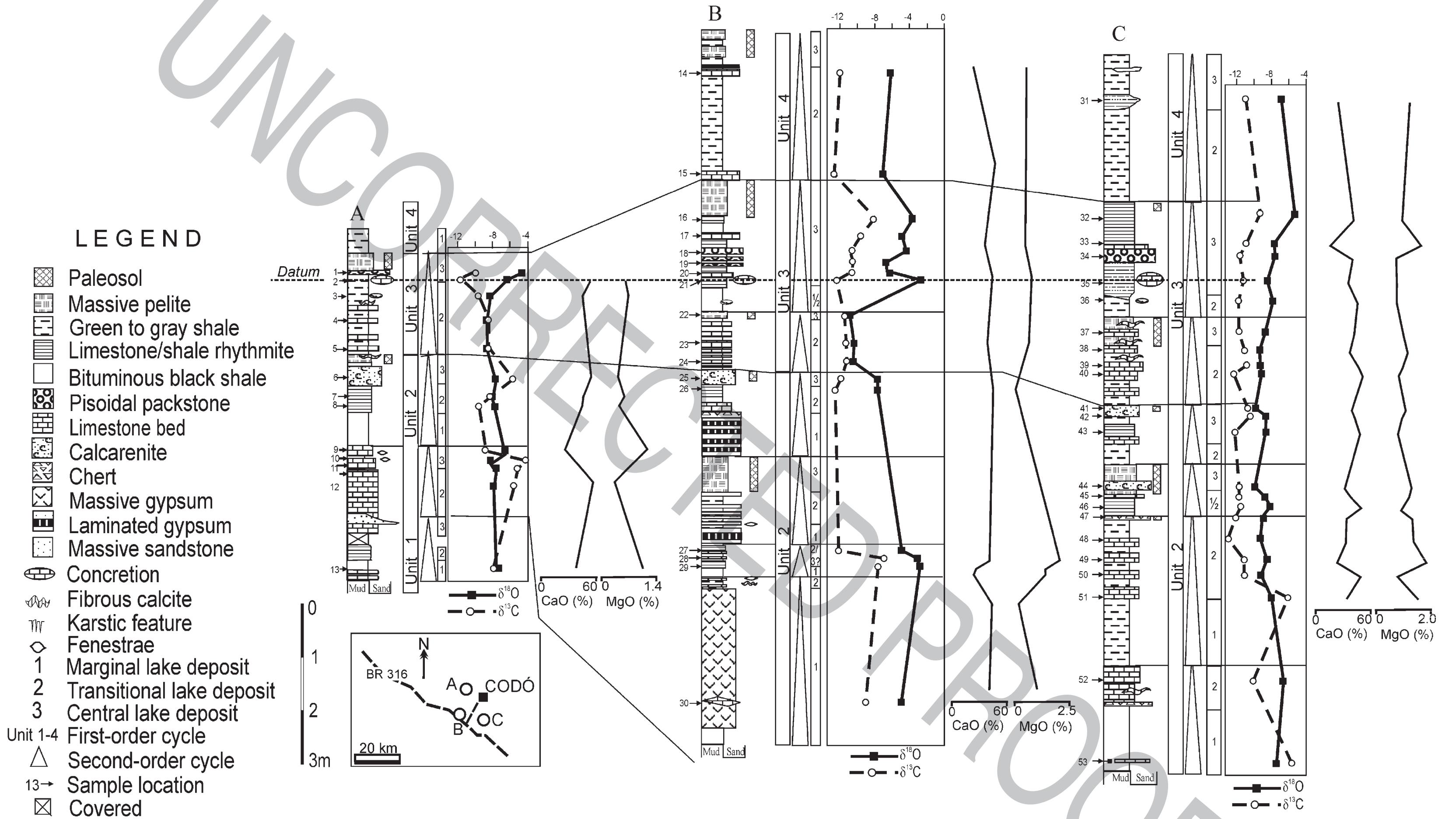

Fig. 8. Lithostratigraphic profiles representative of the Codó Formation exposed in the study area, with the stratigraphic distribution of facies associations, first- and second-order cycles, and $\delta^{18}O$ and $\delta^{13}C$ values, and the contents of CaO and MgO.

Table 1
$\delta^{13}C$ and $\delta^{18}O$ values obtained for the studies deposits

Prof	Sample		$\delta^{18}O$	$\delta^{13}C$
A	01	pisoidal packstone	−5.49	−10.10
	02	ostracodal packstone	−7.24	−11.80
	03	lime_mudstone	−8.91	−10.03
	04	lime_mudstone	−9.17	−9.13
	05	lime_mudstone	−9.15	−8.96
	06	fenestral calcarenite	−8.36	−6.65
	07	ostracodal packstone	−8.45	−9.92
	08	ostracodal packstone	−8.36	−10.92
	09	lime_mudstone	−7.22	−9.26
	10	lime_mudstone	−8.92	−5.15
	11	lime_mudstone	−8.16	−6.09
	12	lime_mudstone	−8.62	−6.31
	13	ostracodal packstone	−8.28	−8.50
B	14	ostracodal packstone	−6.05	−11.99
	15	ostracodal packstone	−7.02	−12.67
	16	ostracodal packstone	−3.39	−7.98
	17	ostracodal packstone	−4.75	−9.6
	18	pisoidal packstone	−4.28	−10.8
	19	ostracodal packstone	−6.62	−10.48
	20	ostracodal packstone	−6.51	−10.71
	21	ostracodal packstone	−5.27	−12.39
	22	lime_mudstone	−10,8	−11.47
	23	lime_mudstone	−10.36	−11.27
	24	lime_mudstone	−10.44	−11.14
	25	lime_mudstone	−7.58	−11.89
	26	ostracodal packstone	−7.6	−12.56
	27	ostracodal packstone	−4.77	−12.16
	28	ostracodal packstone	−3.01	−6.81
	29	ostracodal packstone	−2.71	−7.55
	30	lime_mudstone	−4.80	−9.04
C	31	ostracodal packstone	−6.87	−10.96
	32	ostracodal packstone	−5.32	−9.30
	33	ostracodal packstone	−7.69	−10.95
	34	pisoidal packstone	−7.62	−11.51
	35	ostracodal packstone	−8.38	−11.00
	36	ostracodal packstone	−7.83	−11.87
	37	lime_mudstone	−8.69	−11.72
	38	lime_mudstone	−9.41	−11.03
	39	peloidal packstone	−9.36	−10.89
	40	peloidal packstone	−9.15	−12.38
	41	fenestral calcarenite	−9.83	−10.70
	42	fenestral calcarenite	−8.00	−10.00
	43	ostracodal packstone	−8.64	−12.12
	44	fenestral calcarenite	−994	−11.80
	45	lime_mudstone	−8.83	−11.74
	46	ostracodal packstone	−8.18	−11.57
	47	lime_mudstone	−8.99	−12.12
	48	lime_mudstone	−9.24	−13.02
	49	lime_mudstone	−8.62	−11.23
	50	lime_mudstone	−9.29	−11.18
	51	peloidal packstone	−8.06	−6.10
	52	ostracodal packstone	−6.65	−10.14
	53	ostracodal packstone	−7.42	−5.69
Prof	Sample		$\delta^{18}O$	$\delta^{13}C$
A	cd 319	pisoidal packstone	−5,49	−10,10
	cd 318	ostracodal packstone	−7,24	−11,80
	cd 380	lime_mudstone	−8,91	−10,03
A	cd 321	lime_mudstone	−9,17	−9,13
	cd 313A	lime_mudstone	−9,15	−8,96
	cd 357	fenestral calcarenite	−8,36	−6,65
	cd 356a	ostracodal packstone	−8,45	−9,92
	cd 356b	ostracodal packstone	−8,36	−10,92
	cd 317	lime_mudstone	−7,22	−9,26
	cd 316	lime_mudstone	−8,92	−5,15
	cd 315	lime_mudstone	−8,16	−6,09
	cd 314b	lime_mudstone	−8,62	−6,31
	cd 355	ostracodal packstone	−8,28	−8,50
B	cd 125	ostracodal packstone	−6,05	−11,99
	cd 178	ostracodal packstone	−7,02	−12,67
	cd 177	ostracodal packstone	3,39	−7,98
	cd 166	ostracodal packstone	−4,75	−9,6
	cd 132	pisoidal packstone	−4,28	−10,8
	cd 179	ostracodal packstone	−6,62	−10,48
	cd 167	ostracodal packstone	−6,51	−10,71
	cd 3	ostracodal packstone	−5,27	−12,39
	cd 134	lime_mudstone	−10,8	−11,47
	cd 176	lime_mudstone	−10,36	−11,27
	cd 175	lime_mudstone	−10,44	−11,14
	cd 250	lime_mudstone	−7,58	−11,89
	cd 136	ostracodal packstone	−7,6	−12,56
	cd 158	ostracodal packstone	−4,77	−12,16
	cd 159	ostracodal packstone	−3,01	−6,81
	cd 154	ostracodal packstone	−2,71	−7,55
	cd 162	lime_mudstone	−4,80	−9,04
C	cd 371	ostracodal packstone	−6,87	−10,96
	cd 367	ostracodal packstone	−5,32	−9,30
	cd 368	ostracodal packstone	−7,69	−10,95
	cd 196	pisoidal packstone	−7,62	−11,51
	cd 198	ostracodal packstone	−8,38	−11,00
	cd 364	ostracodal packstone	−7,83	−11,87
	cd 362	lime_mudstone	−8,69	−11,72
	cd 195	lime_mudstone	−9,41	−11,03
	cd 111	peloidal packstone	−9,36	−10,89
	cd 110	peloidal packstone	−9,15	−12,38
	cd 193	fenestral calcarenite	−9,83	−10,70
	cd 199	fenestral calcarenite	−8,00	−10,00
	cd 191	ostracodal packstone	−8,64	−12,12
	cd 192	fenestral calcarenite	−9,94	−11,80
	cd 377	lime_mudstone	−8,83	−11,74
	cd 106	ostracodal packstone	−8,18	−11,57
	cd 112	lime_mudstone	−8,99	−12,12
	cd 375	lime_mudstone	−9,24	−13,02
	cd 101	lime_mudstone	−8,62	−11,23
	cd 84	lime_mudstone	−9,29	−11,18
	cd 121	peloidal packstone	−8,06	−6,10
	cd 189	ostracodal packstone	−6,65	−10,14
	cd 188b	ostracodal packstone	−7,42	−5,69

(Prof = lithostratigraphic profiles as indicated in the Fig. 8).

organic matter, pyrite or pedogenetic influence associated with marginal lake deposits, which are situations that might have naturally affected the iron content during or shortly after deposition, not implying in carbon and oxygen fractionation.

Binary diagrams of trace elements plotted against Ca might be useful for further evaluating the diagenetic influence in limestones. The results revealed that the analysed samples were not significantly modified after deposition, which is particularly suggested by the low correlation of Mn, Sr and Na with respect to Ca (Fig. 7). On the other hand, there is a high inverse correlation between Mg and Ca, which could be interpreted as resulting from diagenesis, when Mg might replace Ca in the carbonate structure. However, considering the non-covariance of the other trace elements, this correlation between Mg and Ca might be related not to diagenesis, but to a change in depositional conditions, probably indicating more evaporative phases. This alternative interpretation is supported here by the fact that the total Mg content increases downward in the sections, where evaporites become more frequent (Fig. 8). Therefore, the good negative correlation between Ca and Mg is related to a change in depositional conditions rather than diagenetic alteration.

6. Results

The $\delta^{13}C$ isotope curves obtained from the studied profiles show values ranging from −5.69‰ to −13.02‰. In general (Table 1), there is no perfect match when all the studied profiles are compared. However, all sections show an overall slight decrease in carbon values, while the oxygen values first decrease and then slightly increase upward (Fig. 8). In addition, the changes in $\delta^{13}C$ isotope values are not random when several intervals of the curves are contrasted, but they have good correspondence within the lowest frequency, shallowing-upward depositional cycles. Hence, unit 2 displays values that, in general, decrease upward, with a tendency for stabilization or slight increase at the top. On the other hand, the carbon values in unit 3 of profiles B and C display an opposed pattern (Fig. 8), varying upward from lighter to heavier. Fluctuations in carbon isotope ratios are variable within individual second-order cycles, but a general trend can be recognized when all sections are contrasted. Hence, it is interesting to observe that the second-order cycles located lower in the sections display carbon values that decrease upward, while up in the sections there is a dominance of cycles with tendency to either increase or increase and then slightly decrease in carbon values.

Similarly to carbon, the oxygen isotope ratios obtained for the Codó Formation are dominantly low, ranging from −2.71‰ to −10.80‰. The behavior of the curves up the profiles within first- and second-order cycles shows patterns that resemble the ones described for the carbon.

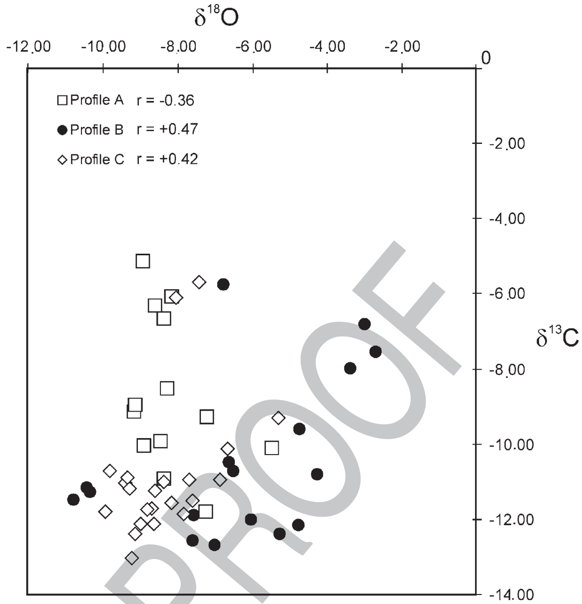

Fig. 9. Correlation curves of carbon and oxygen isotope data from the Codó Formation in the eastern Grajaú Basin. The positive correlation in profiles B and C is attributed to episodes of dominantly closed lake system, while the negative correlation in profile A records lake opening.

Comparisons of carbon and oxygen data from all studied samples revealed that profiles B and C display curves that are, in general, more covariant than profile A (Figs. 8 and 9). In those profiles, however, there are segments with good covariance that alternate with non-covariant intervals, which is reflected by moderate correlation coefficients ranging from +0.42 to +0.47, respectively. Profile A, which is the least covariant, shows an overall negative covariance of −0.36 (Fig. 9).

7. Discussion

The carbon and oxygen data presented here ~~has~~ valuable application for further support of the lacustrine signature of the Codó Formation, as well as reconstruct its paleohydrology and evolution through time. This procedure was made possible only considering the primary signature of these data, as confirmed by the petrographic and geochemical tracers discussed earlier in this paper. In addition, the wide variation of the carbon and oxygen values throughout the analysed profiles and the comparable trends observed among the profiles considering first- and second-order shallowing-upward cycles are more consistent with a depositional control.

Several observations related to the carbon and oxygen isotope data are in agreement with a lacustrine interpretation for the Codó Formation exposed in the eastern margin of the Grajaú Basin, as proposed in previous publications (e.g., Campbell et al., 1949; Aranha et al., 1990; Rossetti et al., 2000; Paz and Rossetti, 2001). First, a non-marine or marginal terrestrial/marine setting is supported by the exclusive occurrence of values lighter than −5.69‰ for the carbon, which is well below the range of about −2‰ and +5‰ expected for marine limestones (e.g., Deines, 1980; Hoefs, 1980). Second, the carbon values obtained in the study area are consistent with Upper Aptian continental influenced deposition, since marine limestones of this age display values ranging from +2‰ to +4‰ (Jones and Jenkins, 2001a,b). Third, the ratios of −2.71‰ to −10.80‰ for the oxygen isotopes are also consistent with a continental setting (Talbot, 1990; Bird et al., 1991). Marine-influenced continental environments might show lighter values of up to −5‰ (e.g., Ingram et al., 1996; Hendry and Kalin, 1997; Fig. 9), but this hypothesis is very unlikely in this instance because 91% of the analysed samples are below this value. Fourth, the overall wide range of both $\delta^{13}C$ and $\delta^{18}O$ values is typical of continental-derived waters, as considered in a number of works (e.g., Talbot and Kelts, 1990; Casanova and ~~Hillaire-~~Marcell, 1993; Camoin et al., 1997; Fig. 10). Fifth, the presence of segments with oxygen and carbon covariant trends (Fig. 10), though not exclusive to, is more consistent with a non-marine setting (Turner et al., 1983; Gasse et al., 1987; Marcell and Casanova, 1987; Talbot, 1990; Talbot and Kelts, 1990; Charisi and Schmitz, 1995). Recent studies focusing on Sr and S isotopes have also arrived to the conclusion that the Codó Formation exposed in the eastern Grajaú Basin was deposited in a dominantly continental setting (Paz et al., 2005).

In addition to supporting a non-marine deposition, the carbon and oxygen isotope data revealed to be valuable for reconstructing lake paleohydrology. Both of these isotopes have been used directly or indirectly to interpret climate. In fact, temperature and hydrologic balance are the main controllers of isotopic composition in lake systems (Kelts and Talbot, 1990; Lister et al., 1991). It is well known from studies of modern settings that temperature causes fractionation of the oxygen in a constant ratio of 0.26‰/°C in the bicarbonate–water–carbonate system (cf. Craig, 1965; Friedman and O'Neill, 1977). The wide range of $\delta^{18}O$ values observed in the Codó Formation, though, would require a

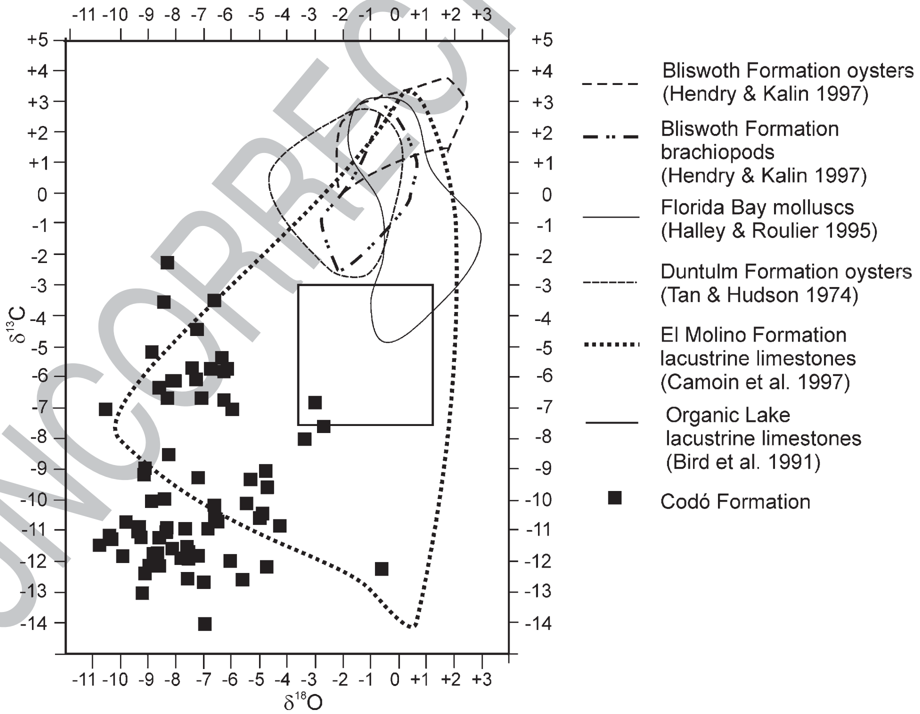

Fig. 10. Plots of carbon and oxygen stable isotope data from several marine and lacustrine deposits throughout the world (modified from Hendry and Kalin, 1997), and their comparison with data obtained in the Codó Formation. This diagram shows that the isotopic composition of the Codó Formation is much more in conformity with isotope data from lacustrine limestones than with marine limestones.

temperature gradient equivalent to about 40 °C, which is not expected considering the low paleolatitudinal location (>10°) of the study area during the ~~Late~~ Aptian (Scotese et al., 1989). On the other hand, the balance between influx and evaporation causes drastic changes in lake isotopic composition (Talbot, 1990; Lister et al., 1991). Evaporation leads to enriched ^{18}O, as lighter ^{16}O escape to the atmosphere. Conversely, high water inflow results in the return of ^{16}O from the atmosphere, causing depletion in $\delta^{18}O$ values. Thus, low $\delta^{18}O$ values have been related to higher lake levels, while high $\delta^{18}O$ are attributed to lower lake levels, parameters that have been indirectly related to climate (e.g., Talbot, 1990; Camoin et al., 1997; Lister et al., 1991).

Carbon isotope ratios also have a direct relation to climate. Hence, higher $\delta^{13}C$ values have been associated with aridity, while lower $\delta^{13}C$ values indicate relatively more humid climates (e.g., Talbot and Kelts, 1990; Valero-Garcés et al., 1995). In general, this interpretation is based on the fact that dry climates favor evaporation, increased influence of C4-path vegetation type, lower influx, and lake stratification, which ultimately lead to organic matter preservation with the consequent output of ^{12}C from lake waters. ~~Except for vegetation type, which has not been adequately studied yet, all~~ these conditions, including a vegetation type dominated by algal components (Mitsuru Arai, oral communication), can be inferred from the sedimentologic characteristics of the Codó Formation, responding, at least in part, to increase the $\delta^{13}C$ values. However, other causes might have been involved in this particular instance, as discussed below.

A close relationship between the carbon and oxygen isotope ratios and the first- and second-order shallowing-upward cycles is recorded in the study area (Fig. 11A–F). These changes are analysed in the following in terms of facies development, which is not necessarily related to climate changes, as widely applied in the literature (e.g., Olsen, 1986; Smoot and Olsen, 1994; ~~Goldsmith et al., 1990;~~ Steenbrink et al., 2000; Hofman et al., 2000; Aziz et al., 2000). In this instance, the good correspondence in both isotope values when first and second-order depositional cycles are compared among the profiles is suggestive of facies control. In particular, the changes from decreasing to either increasing or increasing and then decreasing values in second-order cycles located in the base and top of the profiles, respectively, can be related to the presence of either complete or incomplete cycles with well developed marginal lake deposits upward in the sections. Such facies stacking requires alternating episodes of lake deepening and shallowing, which in this instance is associated with increased subsidence (Fig. 11A, C, E) and the return to relative stability or even uplift (Fig. 11B, D, F), respectively, as previously mentioned. Heavier isotope values recorded during shallowing could be attributed to a significant enhancement of the isotopic exchange between the lake surface and the atmosphere. This is because as the water became extremely shallow, evaporation increased significantly due to heating. Differences in carbon values according to location in the lake system, with marginal areas displaying higher values, have been also noted by other authors (e.g., Camoin et al., 1997; Casanova and ~~Hillaire-~~Marcell, 1993). The loss of ^{12}C to the atmosphere leading to enrichment in the ^{13}C in the dissolved inorganic carbonate appears to be an active process in the epilimnion of lakes with low water inflow (Stiller et al., 1985; Talbot, 1990; Talbot and Kelts, 1990). The cycles located up in the sections that display an increase and then a slight decrease in values probably record extreme shallowing, which culminated with periods of desiccation, as indicated by deposits with paleosols. During subaerial exposure, there is a greater chance that the deposits were in contact with meteoric waters, which might have brought lighter carbon and oxygen, contributing to decrease the isotope values.

A facies control on the isotope values obtained from the study area is also consistent with the corresponding trends obtained for the curves when first-order cycles are compared among all the profiles. As presented earlier, these cycles record main episodes of lake desiccation superposed upon the second-order cycles, in this instance associated with decreasing subsidence. Hence, the overall decreasing values observed throughout the first-order depositional unit 2 would reflect a period when the lake was established, with deeper water lake deposits prevailing over shallower water lake deposits, which resulted in low isotope values. Marginal lake deposits that could record ~~increased~~ evaporation, contributing to increase the isotope values through atmosphere exchange, as proposed above are, in general, lacking in the upper portions of this unit. As the lake evolved, increased evaporation decreased the water level, and progressively enhanced the isotope values, a trend exemplified by depositional unit 3. Decreasing subsidence during deposition of this unit would have promoted a better development of marginal lake deposits, and the consequent maximum isotope values.

Pulses with heavier carbon isotope values observed in the middle portion of depositional unit 2 could be related to lake stratification and bottom anoxia. The mechanism responsible for sulphate precipitation in this

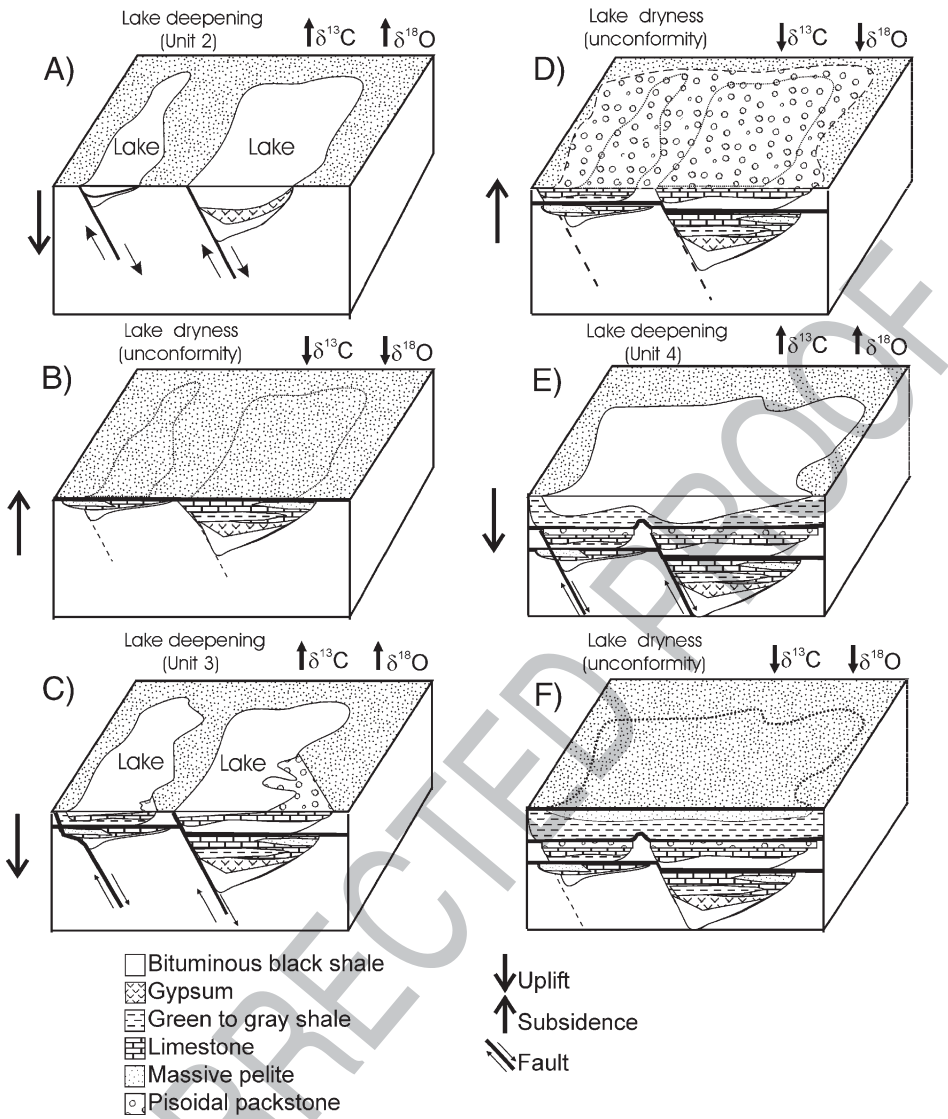

Fig. 11. Summary of the depositional model proposed for ~~the origin of~~ the Codó lake system in the eastern Grajaú Basin, illustrating the close relationship of facies development, and thus the distribution of oxygen and carbon isotopes, with alternation between syn-sedimentary fault displacement and uplift. (A) Offset of few meters along faults ~~displaced along~~ the basin margins resulted in ~~the~~ creation of accommodation space along subsiding areas, where the lake system developed, giving rise to first-order cycle represented by unit 2. (B) Uplift contributed to decrease the lake level with the consequent spread out of marginal deposits at the top of unit 2, culminating with lake dryness and formation of a discontinuity surface with paleosols. (C) Fault reactivation resulted in a renewed phase of lake deepening, with deposition of central and transitional facies deposits recorded by unit 3. (D) Renewed uplift promoted ~~the~~ fall in lake level and widespread formation of marginal deposits represented by pisoidal packstone to grainstone and rhythmite, which culminated with lake exposure and soil development at the top of unit 3. (E) Fault reactivation with renewed deposition of laminated argillites, recorded by unit 4. (F) Increas~~ing~~ stability led to progressive decrease in water level resulting from the abandonment of the lacustrine deposition in the study area, with subaerial exposure and formation of an unconformity at the top of the Codó Formation.

type of setting is not well understood yet, but stagnating, disaerobic environments are naturally enriched in dissolved sulphates. These might precipitate under increased evaporation (Burns et al., 2000; Dell Cura et al., 2001), resulting in large gypsum deposits interbedded with black shales, as commonly recorded in many other central lake settings throughout the world (e.g., Kirkland and Evans, 1981; Warren, 1999; Landmann et al., 2002). An important point to highlight concerning the carbon isotope behavior under such environmental condition is that continuing sedimentation leads to ^{12}C burial, consequently increasing the amount of ^{13}C dissolved in central lake waters (Herczeg, 1988; Talbot and Kelts, 1990). If this interpretation is considered, then the subtle upward decrease in carbon isotope values could be attributed to ~~the~~ gradation from central to transitional lake environments, where this effect was less significant.

The moderate positive covariance between the carbon and oxygen isotope curves shown in profiles B and C are attributed to periods with a tendency for lake closure (Fig. 9). Covariance between carbon and oxygen isotope values is an attribute verified in many other ancient and modern lake systems throughout the world (e.g., Eicher and Siegenthaler, 1976; Gat, ~~1981~~; Gasse et al., 1987; Gasse et al., 1989; McKenzie, 1985; Janaway and Parnell, 1989; Talbot, 1990; Talbot and Kelts, 1990; Lister et al., 1991). This occurs because, as the system remains closed, the supply of ^{16}O and ^{13}C to the basin is greatly reduced. No external inflow, added to an increase in residence time, resulted in the consequent release of ^{16}O and ^{13}C to the atmosphere due to evaporation, particularly considering arid climates as envisaged for the study area during the ~~Late~~ Aptian. This process might have contributed to further increase the isotope values in this instance. The alternation of covariant and non-covariant carbon and oxygen values, however, which resulted in correlation coefficients ranging from +0.42 to +0.47 in these profiles, suggest moments of lake opening. Such situation appears to have dominated the deposition of profile A, which is the least covariant. The fact that sandstones occur only in this profile (see Fig. 8, base of profile A) is consistent with a lake connected, at least temporarily, to a sand influx.

It is noteworthy that the $\delta^{18}O$ values displayed the highest variation during closed phases, ranging from −3.63‰ to −4.89‰, compared to the variations of −0.09‰ to −1.87‰ that characterize open phases. This is because closed lakes have a better chance to show oscillations in water levels, due to the increase in residence time as explained above, leading to higher $\delta^{18}O$ values. Conversely, the isotopic composition of open lakes is more stable due to the balance caused by the continuous basin inflow, as recorded in several lake systems, such as Lake Henderson (Stuiver, 1970), Lake Huleh (Stiller and Hutchinson, 1980) and Lake Greifensee (McKenzie, 1985).

8. Final remarks

The carbon and oxygen isotopic composition of carbonates in the Codó Formation in the eastern Grajaú Basin can be directly related to facies changes, as revealed by the correspondence between the isotope values and the shallowing-upward cycles when all the profiles are compared. Deciphering the causes of these changes through time, whether related to climate fluctuations or to any other variations in the basin, such as subsidence or sediment inflow, is not so straightforward. There has been an agreement among ~~the~~ authors in relating carbon and oxygen isotopes with lake hydrology, which is often used directly or indirectly to make inferences about climate (e.g., Smoot and Olsen, 1994; Steenbrink et al., 2000; Hofman et al., 2000; Aziz et al., 2000). In study this is not the case and significant changes in carbon and oxygen isotope composition of lake waters, resembling climatic cycles, can be related to fluctuations in subsidence rates caused by syn-sedimentary seismic activity. ~~In this case, the combination~~ of isotope and sedimentological data provides the key for distinguishing which of these factors left the most significant imprint in the sedimentary record.

In this paper~~,~~ we have shown the close relationship of both carbon and oxygen isotopes with the first- and second-order shallowing-upward cycles that characterize the studied unit. The dominant asymmetric nature of these cycles, inferred on the basis of high facies variability when comparing one cycle to another, the limited lateral extension, as well as the frequent and random thickness changes, lead us to propose that climate was not their prime controlling factor. On the other hand, sedimentological data favors the attribution of these cycles to syn-sedimentary seismic activity associated with the early tectonic evolution of the São Luís-Grajaú Basin during the Late Aptian. The Codó Formation was deposited just prior to the main rifting that culminated in the process of opening of the South Atlantic Equatorial Ocean. During this initial time, there was the development of a shallow, but extensive subsiding intracontinental basin (Azevedo, 1991; Góes and Rossetti, 2001). This suggestion matches well with the presence of shallow lakes in marginal areas of the basin, where faults with reduced offsets are expected to have prevailed. Subsidence gave rise to local water accumulation, forming closed and perennial lake systems, but as compression took place, and the area was uplifted, the development of ephemeral lakes appears to have been favored. This situation is recorded in the studied profiles by a change from shallowing-upward cycles with dominance of central and transitional lake deposits to cycles with well-developed marginal lake deposits, as occurs in the lower and upper portions of the first-order cycles, respectively. Such facies arrangement records the upward transition from periods of maximum flooding to periods when the lake fell to lower levels. The carbon and oxygen isotopic composition of such lake basins is expected to be characterized initially by light values, but as the residence time increases due to shallowing, heavier values are reached due to increased evaporation in a shallowing lake.

Because an arid climate prevailed along the Brazilian equatorial margin during the ~~Late~~ Aptian (Lima et al., 1980; Lima, 1982; Batista, 1992; Rodrigues, 1995; Rossetti et al., 2001), gypsum precipitation took place in central lake areas, a process that was probably induced by water stratification and bottom anoxia. The highest carbon isotope values coinciding with the moment of maximum formation of gypsum and bituminous black shales are consistent with this interpretation.

Therefore, different styles and/or intensities of seismic pulses alternating with sediment deposition might cause changes in the lake level, promoting alternating periods of rise and fall in lake level, and resulting in well-developed asymmetric shallowing-upward cycles. Such a scenario ultimately affects the overall isotope composition of lake waters.

9. Uncited references

Gat, 1980
Gat, 1984
Tan and Hudson, 1974

Acknowledgments

The Itapicuru Agroindustrial S/A is acknowledged for the permission to access the quarries with the exposures of the Codó Formation. This work was financed by the Brazilian Council for Research-CNPq (Project #460252/01). The authors are grateful to Dr. Alcides Sial and Dr. Valderez Ferreira for helping with the geochemical analysis. The anonymous reviewers are thanked for the numerous suggestions and corrections that have contributed to substantially improve the final version of the manuscript.

References

Abell, P.I., Williams, M.A.J., 1986. Sedimentary carbonates as isotopic marker horizons at Lake Turkana, Kenya. In: Frostick, L.E., Renaut, R.W., Reid, I., Tiercelin, J.-J. (Eds.), Sedimentation in the African Rifts. Spec. Publ., Geol. Soc. Am., 25, pp. 153–158.

Anderson, F.W., Arthur, M.A., 1983. Stable isotopes of oxygen and carbon and their application to sedimentologic and paleoenvironmental problems. Short Course Notes, SEPM, 10. 151 pp.

Aranha, L.G., Lima, H.P., Makino, R.K., Souza, J.M., 1990. Origem e evolução das bacias de Bragança-Viseu, São Luís e Ilha Nova. In: Milani, E.J., Raja Gabaglia, G.P. (Eds.), Origem e Evolução das Bacias Sedimentares. PETROBRAS, Rio de Janeiro, pp. 221–234.

Azevedo, R.P., 1991. Tectonic evolution of Brazilian Equatorial Continental Margin Basins. Doctoral Thesis. University of London, London. 455 pp.

Aziz, H.A., Hilgen, F., Krijgsman, W., Sanz, E., Calvo, J.P., 2000. Astronomical forcing of sedimentary cycles in the middle to late Miocene continental Catalayud Basin (NE Spain). Earth Planet. Sci. Lett. 177, 9–22.

Batista, A.M.N., 1992. Caracterização Paleoambiental dos sedimentos Codó-Grajaú, Bacia de São Luís (MA). M.Sc.Thesis, Universidade Federal do Pará, Belém. 102 pp.

Bellanca, A., Calvo, J.P., Censi, P., Elizaga, E., Neri, R., 1989. Evolution of lacustrine diatomite carbonate cycles of Miocene age, southeastern Spain: petrology and isotope geochemistry. J. Sediment. Petrol. 59, 45–52.

Benvenuti, M., 2003. Facies analysis and tectonic significance of lacustrine fan-deltaic successions in the Pliocene–Pleistocene Mugello Basin, Central Italy. Sediment. Geol. 157, 197–203.

Bird, M.I., Chivas, A.R., Radnell, C.J., Burton, H.R., 1991. Sedimentological and stable isotope evolution of lakes in the Vestfold Hills, Antarctica. Palaeogeogr. Palaeoclimatol. Palaeoecol. 84, 109–130.

Burns, S.J., McKenzie, J.A., Vasconcelos, C., 2000. Dolomite formation and biogeochemical cycles in the Phanerozoic. Sedimentology 47, 49–61.

Camoin, G., Casanova, J., Rouchy, J.M., Blanc-Valleron, M.M., Deconinck, J.F., 1997. Environmental controls on perennial and ephemeral carbonate lakes: the Central Palaeo-Andean Basin of Bolivia during Late Cretaceous to early Tertiary times. Sediment. Geol. 113, 1–26.

Campbell, D.F., Almeida, L.A., Silva, S.O., 1949. Relatório preliminar sobre a geologia da Bacia do Maranhão. Bol. Cons. Nac. Petról. 1, 1–160.

Casanova, J., Hillaire-Marcell, C, 1993. Carbon and oxygen isotopes in African lacustrine stromatolites: palaeohydrological interpretation. In: Swart, P.K., Lohmann, K.C., McKenzie, J., Savin, S. (Eds.), Climate Change in Continental Isotopic Record. Geophys. Monogr., Am. Geophys. Union, vol. 94, pp. 123–133.

Charisi, S.D., Schmitz, B., 1995. Stable (^{13}C, ^{18}O) and strontium (^{87}Sr/^{86}Sr) isotopes through the Paleocene et Gebel Aweina, eastern Tethyan region. Palaeogeogr. Palaeoclimatol. Palaeoecol. 116, 103–129.

Craig, H., 1965. The measurement of oxygen isotope palaeotemperatures. In: Tongiorgi (Ed.), Stable Isotopes in Oceanographic Studies and Palaeotemperatures. Cons. Naz. Rich. Lab. Geol. Nucl., Pisa, pp. 9–130.

Deines, P., 1980. The isotopic composition of reduced organic carbon. In: Fritz, P.J., Fontes, J. (Eds.), Handbook of Environmental Isotope Geochemistry. Terrestrial Environment, vol. 1. Elsevier, Amsterdam, pp. 329–406.

Dell Cura, M.A.G., Calvo, J.P., Ordóñez, S., Jones, B.F., Cañaveras, J. C., 2001. Petrographic and geochemical evidence for the formation of primary, bacterially induced lacustrine dolomite: La Roda 'white earth' (Pliocene, central Spain). Sedimentology 48, 897–915.

Eicher, U., Siegenthaler, U., 1976. Palynological and oxygen isotope investigations on Late-Glacial sediment cores from Switzerland. Boreas 5, 109–117.

Friedman, I., O'Neill, J.R., 1977. Compilation of stable isotope fractionation factors of geochemical interest. In: Fleischer, M.

(Ed.), Data of Geochemistry. U.S. Gov. Print. Office, Washington, pp. 1–12. Geological survey Prof. Paper 440-KK.

Gasse, F., Fontes, J.C., Plaziat, J.C., Carbonel, P., Kaczmarska, I., De Decker, P., Soulié-Marsche, I., Callot, Y., Depeuble, P.A., 1987. Biological remains, geochemistry and stable isotopes for the reconstruction of environmental and hydrological changes in the Holocene lakes from north Sahara. Palaeogeogr. Palaeoclimatol. Palaeoecol. 60, 1–46.

Gasse, F., Lédée, V., Massault, M., Fontes, J.C., 1989. Water-level fluctuations of Lake Tanganyika in phase with the oceanic changes during the last glaciation and deglaciation. Nature 342, 57–59.

Gat, J.R., 1980. The isotopes of hydrogen and oxygen in precipitation. In: Fritz, P.J., Fontes, J. (Eds.), Handbook of Environmental Isotope Geochemistry. . Terrestrial Environment, vol. 1. Elsevier, Amsterdam, pp. 21–47.

Gat, J.R., 1984. The stable isotope composition of Dead Sea waters. Earth Planet. Sci. Lett. 71, 361–376.

Góes, A.M., Rossetti, D.F., 2001. Gênese da Bacia de São Luís-Grajaú. In: Rossetti, D.F., Góes, A.M., Truckenbrodt, W. (Eds.), O Cretáceo na Bacia de São Luís Grajaú. Museu Paraense Emilio Goeldi, Coleção Friedrich Katzer, Belém, pp. 15–29.

Goldhammer, R.K., Dunn, P.A., Hardie, L.A., 1990. Depositional cycles, composite sea-level changes cycle stacking patterns, and hierarchy of stratigraphic forcing: examples from Alpine Triassic platform carbonates. Geol. Soc. Am. Bull. 102, 535–562.

Hendry, J.P., Kalin, R.M., 1997. Are oxygen and carbon isotopes of mollusc shells reliable palaeosalinity indicators in marginal marine environments? A case study from Middle Jurassic of England. J. Geol. Soc. London 154, 321–333.

Herczeg, A.L., 1988. Early diagenesis of organic matter in lakes sediments: a stable carbon isotope study of pore waters. Chem. Geol. 72, 199–209.

Herczeg, A.L., Leaney, F.W., Dighton, J.C., Lamontagne, S., Schiff, S. L., Telfer, A.L., English, M.C., 2003. A modern isotope record of changes in water and carbon budgets in a groundwater-fed lake: Blue Lake, South Australia. Limnol. Oceanogr. 48, 2093–2105.

~~Hillaire-~~Marcell, C., Casanova, J., 1987. Isotopic hydrology and paleohydrology of the Magadi (Kenya)-Natron (Tanzania) basin during Late Quaternary. Paleogeogr. Paleoclimatol. Paleoecol. 58, 155–181.

Hoefs, J., 1980. Stable Isotope Geochemistry, 2nd Ed. Springer-Verlag, Berlim. 208 pp.

Hofman, A., Tourani, A., Gaupp, R., 2000. Cyclicity of Triassic to lower Jurassic continental red beds of the Argana Valley, Morocco: implications for paleoclimate and basin evolution. Palaeogeogr. Palaeoclimatol. Palaeoecol. 161, 229–266.

Holland, H.D., 1978. The Chemistry of the Atmosphere and Oceans. Wiley-Interscience, New York. 351 pp.

Ingram, B.L., Ingle, J.C., Conrad, M.E., 1996. A 2000-yr record of Sacaramento-San Joaquin River inflow to the San Francisco Bay estuary, California. Geology 24, 331–334.

In Sung, P., Kim, H.J., 2003. Palustrine calcretes of the Cretaceous Gyeongsang Supergroup, Korea: variation and paleoenvironmental implications. The Island Arc 12, 110–124.

Janaway, T.M., Parnell, J., 1989. Carbonate production within the Orcadian Basin, northern Scotland: a petrographic and geochemical study. In: Talbot, M.R., Kelts, K. (Eds.), The Phanerozoic Record of Lacustrine Basins and their Environmental Signals. Palaeogeogr. Palaeoclimatol. Palalaeoecol., vol. 70, pp. 89–105.

Jones, C.E., Jenkins, H.C., 2001a. Seawater strontium isotopes, oceanic anoxic events, and seafloor hydrothermal activity in the Jurassic and Cretaceous. Am. J. Sci. 301, 112–149.

Jones, C.E., Jenkins, H.C., 2001b. Seawater strontium isotopes, oceanic anoxic events, and seafloor hydrothermal activity in the Jurassic and Cretaceous. Am. J. Sci. 301, 112–149.

Katz, A., Kolodny, Y., Nissenbaum, A., 1977. The geochemical evolution of Lake Lisan–Dead Sea system. Geochim. Cosmochim. Acta 41, 1609–1626.

Kirkland, D.W., Evans, R., 1981. Source-rock potential of evaporitic environment. AAPG Bull. 65, 181–190.

Kelts, K., Talbot, M., 1990. Lacustrine carbonates as geochemical archives of environmental change and biotic/abiotic interactions. In: Tilzer, M.M., Serruya, C. (Eds.), Large lakes: Ecological Structure and Function. Brock/Springer Series in Contemporary Bioscience. Springer-Verlag, pp. 288–315.

Landmann, G., Abu Qudaira, G.M., Shawabkeh, K., Wrede, V., Kempe, S., 2002. Geochemistry of the Lisan and Damya Formations in Jordan and implications for paleoclimate. Quat. Int. 89, 45–57.

Lima, M.R., 1982. Palinologia da Formação Codó, Maranhão. Bol. Inst. Geociênc., USP 13, 116–128.

Lima, M.R., Fulfaro, V.J., Bartorelli, A., 1980. Análise palinológica de sedimentos cretáceos da região de Marabá, Estado do Pará. Bol. Inst. Geociênc., USP 11, 55–161.

Lister, G.S., Kelts, K., Chen, K.Z., Yu, J.-Q., Niessen, F., 1991. Lake Qingai, China: closed-lake basin levels and the oxygen isotope record for ostracoda since the latest Pleistocene. Palaeogeogr. Palaeoclimatol. Palaeoecol. 84, 141–162.

Martel, A.T., Gibling, M.R., 1991. Wave-dominated lacustrine facies and tectonically controlled cyclicity in the Lower Carboniferous Horton Bluff Formation, Nova Scotia Canada. In: Anadón, P., Cabrera, Ll., Kelts, K. (Eds.), Lacustrine Facies Analysis. Int. Assoc. Sediment. Spec. Publ., vol. 13, pp. 223–244.

McKenzie, J.A., 1985. Carbon isotopes and productivity in the lacustrine and marine environment. In: Stumm, W. (Ed.), Chemical Processes in Lakes. Wiley, New York, pp. 99–118.

Mesner, J.C., Wooldrigde, L.C.P., 1964. Maranhão Paleozoic Basin and Cretaceous coastal basins, north Brazil. AAPG Bull. 48, 1475–1512.

Olsen, P.E., 1986. A 40-million-year lake record of Early Mesozoic orbital climatic forcing. Science 234, 842–848.

Paz, J.D.S., Rossetti, D.F., 2001. Reconstrução paleoambiental da Formação Codó (Aptiano), borda leste da Bacia do Grajaú, MA. In: Rossetti, D.F., Góes, A.M., Truckenbrodt, W. (Eds.), O Cretáceo na Bacia de São Luís-Grajaú. Museu Paraense Emilio Goeldi, Coleção Friedrich Katzer, Belém, pp. 77–101.

Paz, J.D.S., Rossetti, D.F., 2005. Linking lacustrine cycles with syn-sedimentary tectonic episodes: an example from the Codó Formation (Late Aptian), northeastern Brazil. Geol. Mag. 142, 269–285.

Paz, J.D.S., Rossetti, D.F., Macambira, M.J.B., 2005. An Upper Aptian saline pan/lake system from the Brazilian Equatorial Margin: integration of facies and isotopes. Sedimentology 52, 1303–1321.

Rezende, W.M., Pamplona, A.H.R.P., 1970. Estudo do desenvolvimento do Arco Ferrer-Urbano Santos. PETROBRAS, Boletim Técnico 13, 5–14.

Rodrigues, R., 1995. A geoquímica Orgânica na Bacia do Parnaíba. Doctoral Thesis, Universidade Federal do Rio Grande do Sul, Porto Alegre, 225 pp.

Rosenmeier, M.F., Hodell, D.A., Brenner, M., Curtis, J.H., Guilderson, T.P., 2002. A 4000-year lacustrine record of environmental change in the Southern Maya Lowlands, Petén, Guatemala. Quat. Res. 57, 183–190.

Rossetti, D.F., 2001. Arquitetura deposicional da Bacia de São Luís-Grajaú, meio norte do Brasil. In: Rossetti, D.F., Góes, A.M., Truckenbrodt, W. (Eds.), O Cretáceo na Bacia de São Luís Grajaú. Museu Paraense Emilio Goeldi, Coleção Friedrich Katzer, Belém, pp. 31–46.

Rossetti, D.F., Góes, A.M., 2000. Deciphering the sedimentological imprints of paleoseismic events: an example from the Codó Formation, northern Brazil. Sediment. Geol. 135, 137–156.

Rossetti, D.F., Truckenbrodt, W., 1997. Classificação estratigráfica para o Albiano-Terciário Inferior (?) na Bacia de São Luís, MA. Boletim do Museu Paraense Emílio Goeldi (Série Ciências da Terra) 9, 31–43.

Rossetti, D.F., Paz, J.D., Góes, A.M., Macambira, M., 2000. A marine versus non-marine origin for the Aptian–Albian evaporites of the São Luís and Grajaú basins, Maranhão state (Brazil) based on sequential analysis. Rev. Bras. Geocienc. 30, 642–645.

Rossetti, D.F., Truckenbrodt, W., Santos-Júnior, A.E., 2001. Clima do Cretáceo no Meio-Norte brasileiro. In: Rossetti, D.F., Góes, A.M., Truckenbrodt, W. (Eds.), O Cretáceo na Bacia de São Luís Grajaú. Museu Paraense Emilio Goeldi, Coleção Friedrich Katzer, Belém, pp. 67–76.

Rossetti, D.F., Paz, J.D., Góes, A.M., 2004. Facies analysis of the Codó Formation (Late Aptian) in the Grajaú area, southern São Luís-Grajaú Basin. An. Acad. Bras. Cienc. 76, 791–806.

Russell, J.M., Johnson, T.C., Talbot, M.R., 2003. A 725-yr cycle in the climate of Central Africa during the Late Holocene. Geology 31, 677–680.

Scotese, C.R., Gahagan, L.M., Larson, R.L., 1989. Plate tectonic reconstructions of the Cretaceous and Cenozoic ocean basins. In: Scotese, C.R., Sager, W.W. (Eds.), Mesozoic and Cenozoic Plate Reconstructions. Elsevier, Amsterdam, pp. 22–48.

Smoot, J.P., Olsen, P.E., 1994. Climatic cycles as sedimentary controls of rift-basin lacustrine deposits in the Early Mesozoic Newark Basin based on continuous core. In: Lomando, A.J., Schreiber, B. C., Harris, P.M. (Eds.), Lacustrine Reservoirs and Depositional Systems. SEPM Core Workshop, vol. 19, pp. 239–295.

Steenbrink, J., Van Vugt, N., Kloosterboer-Van Hoeve, M.L., Hilgen, F.J., 2000. Refinement of the Messinian APTS from sedimentary cycle patterns in the lacustrine Lava section (Servia Basin, NW Greece). Earth Planet. Sci. Lett. 181, 161–173.

Stiller, M., Hutchinson, G.E., 1980. The waters of Meron: a study of Lake Huleh, 1. Stable isotopic composition of carbonates of 54 m core: paleoclimatic and paleotrophic implications. Arch. Hydrobiol. 89, 275–302.

Stiller, M., Rounick, J.S., Shasha, S., 1985. Extreme carbon-isotope enrichments in evaporating brines. Nature 316, 434–435.

Stuiver, M., 1970. Oxygen and carbon isotope ratios of fresh-water carbonates as climatic indicator. J. Geophys. Res. 75, 5247–5257.

Szulc, J., Roger, Ph., Mouline, M.P., Lenguin, M., 1991. Evolution of lacustrine systems in the Tertiary Narbonne Basin, Northern Pyrenean foreland, Southeast France. In: Anadón, P., Cabrera, Ll., Kelts, K. (Eds.), Lacustrine Facies Analysis. Spec. Publ. Int. Ass. Sediment., vol. 13, pp. 279–290.

~~Tan, F.C., Hudson, J.D., 1974. Isotopic studies on the palaeoecology and diagenesis of the Great Estuarine Series (Jurassic) of Scotland. Scott. J. Geol. 10, 91–128.~~

Talbot, M.R., 1990. A review of the paleohydrological interpretation of carbon and oxygen isotopic ratios in primary lacustrine carbonates. Chem. Geol. 80, 261–279.

Talbot, M.R., Kelts, K., 1990. Paleolimnological signatures from carbon and oxygen isotopic ratios in carbonates from organic carbon-rich lacustrine sediments. In: Katz, B.J. (Ed.), Lacustrine Basin Exploration: Case Studies and Modern Analogs. AAPG Memoir, vol. 50, pp. 99–112.

Tucker, M.E., Wright, V.P., 1990. Carbonate Sedimentology. Blackwell Science, Oxford. 482 pp.

Turner, J.V., Fritz, P., Karrow, P.F., Warner, B.G., 1983. Isotopic and geochemical composition of marl lake waters and implications for radiocarbon dating of marl lake sediments. Can. J. Earth Sci. 20, 599–615.

Valero-Garcés, B.L., Kelts, K., Ito, E., 1995. Oxygen and carbon isotopes trends and sedimentological evolution of a meromictic and saline lacustrine system: the Holocene Medicine Lake basin, North American Great Plains, USA. Palaeogeogr. Palaeoclimatol. Palaeoecol. 177, 253–278.

Warren, J.K., 1999. Evaporites: Their Evolution and Economics. Blackwell Scientific, Oxford. 438 pp.